isvr Institute of Sound and Vibration Research

# Analytical Models describing the Coupling between Piezoactuators and a Beam

**G. Gatti, M.J. Brennan and P. Gardonio**

ISVR Technical Memorandum No 923

October 2003

University of Southampton

# SCIENTIFIC PUBLICATIONS BY THE ISVR

***Technical Reports*** are published to promote timely dissemination of research results by ISVR personnel. This medium permits more detailed presentation than is usually acceptable for scientific journals. Responsibility for both the content and any opinions expressed rests entirely with the author(s).

***Technical Memoranda*** are produced to enable the early or preliminary release of information by ISVR personnel where such release is deemed to the appropriate. Information contained in these memoranda may be incomplete, or form part of a continuing programme; this should be borne in mind when using or quoting from these documents.

***Contract Reports*** are produced to record the results of scientific work carried out for sponsors, under contract. The ISVR treats these reports as confidential to sponsors and does not make them available for general circulation. Individual sponsors may, however, authorize subsequent release of the material.

UNIVERSITY OF SOUTHAMPTON

INSTITUTE OF SOUND AND VIBRATION RESEARCH

DYNAMICS GROUP

# Analytical Models Describing the Coupling Between Piezoactuators and a Beam

by

**G. Gatti, M.J. Brennan and P. Gardonio**

ISVR Technical Memorandum No: 923

October 2003

Authorised for issue by
Professor M.J. Brennan
Group Chairman

# Abstract

This report presents a review of the coupling between piezoelectric actuators and a beam. The properties and definitions of piezoelectric materials are briefly discussed and the one-dimensional perfect bonded wafer configuration is analysed. Two configurations are considered: two piezoactuators symmetrically bonded to the upper and lower surface of a beam which can be driven in-phase or out-of-phase with respect to each other and a single piezoactuator bonded to one surface of a beam. After making some assumptions, strain and stress distribution is determined for each case and an expression for the effective load is thus given. The complex beam-actuator structure can then be analysed as a simple structure (the beam) subjected to an equivalent or effective load, which depends on the piezoelectric actuator properties and the coupling.

# Table of Contents

# 1. Introduction

Piezoelectric materials exhibit an interesting property: upon mechanical strain a charge proportional to this is produced. This is referred to as the direct piezoelectric effect [1]. Conversely they also exhibit an inverse piezoelectric effect, whereby upon the application of a voltage (electric charge) a mechanical strain is induced in the material.

Piezoelectric materials, which are designed to use the direct piezoelectric effect, are referred to as sensors, while those designed to use the inverse effect are referred to as actuators. Piezo-actuators and sensors are produced as thin structures that can be shaped for more convenient use. These piezo-actuator/sensor patches are usually bonded directly on the structure whose motion is to be controlled/detected. However, some applications use the transducers embedded inside the structure itself in the manufacturing process [2].

In recent years, research has been devoted to developing active noise and vibration control techniques using piezo-actuators and sensors. Piezoelectric transducers are relatively inexpensive, lightweight, easily shaped and can be bonded to or embedded into a variety of surfaces.

Research efforts are also devoted to the design of electric voltage transformers, which combine both the direct and inverse effect of piezoelectric transducers [3~5]. In order to investigate the coupling of a piezoactuator and a substructure, a number of models have been developed to predict the interaction between induced strain actuators and the structure to which they are bonded.

The objective of this work is to present and review a detailed model developed earlier by Fuller [6] and Kim [7], pointing out the assumptions and limitations employed. Comments and comparisons are made of the cases presented.

## 2. Piezoelectric Materials and Definitions

The piezoelectric effect was first discovered in 1880 by Pierre and Jacques Curie who demonstrated that when a stress field is applied to certain crystalline materials, an electrical charge is produced on the material surface [1]. It was subsequently demonstrated that the converse effect is also true: when an electrical field is applied to a piezoelectric material it changes its shape and size. This effect was found to be due to the electrical dipoles of the material spontaneously aligning in the electrical field. Due to the internal stiffness of the material, piezoelectric elements were also found to generate relatively large forces when their natural expansion or contraction is constrained. This observation has led to their use as actuators in many applications. Likewise if electrodes are attached to the surfaces of the material then the charge generated by straining or stretching the material can be collected and measured. Thus piezoelectric materials can also be used as sensors to measure structural motion by directly attaching them to a structure. Recent applications use polycrystalline ceramics instead of naturally occurring piezoelectric crystals. The electrical properties of the ceramics can be precisely oriented by "poling" the material. The relationships between the applied forces and the resultant response of piezoelectric materials depends upon a number of parameters such as the piezoelectric properties of the material, its size and shape and the direction in which forces or electrical fields are applied relative to the material axis.

Three axes are used to identify directions in the piezoelectric element (Figure 1) termed 1, 2 and 3 in correspondence with the $x$, $y$ and $z$ axes of a rectangular coordinate system. These axes are set during the poling process, which induces the piezoelectric properties of the materials by applying a large DC voltage to the element with the temperature being raised to above the Curie temperature. The $z$-axis is taken parallel to the direction of polarization $p$.

Piezoelectric coefficients, usually written in a form of double subscripts, provide the relationship between electrical and mechanical quantities. The first subscript gives the direction of the electrical fields associated with the voltage applied or the charge produced. The second subscript gives the direction of the mechanical strain.

The constitutive equation for a linear piezoelectric material when the applied electric field and the generated stress are not large, can be written as:

$$\varepsilon_i = C_{ij}\sigma_j + d_{mi}E_m \tag{1.a}$$

$$D_m = d_{mi}\sigma_i + \xi_{ik}E_k \tag{1.b}$$

where the indices $i$, $j$=1,2..6 and $m$, $k$=1,2,3 refer to the different directions within the material coordinate system, 4, 5 and 6 corresponding to $y$-$z$, $z$-$x$ and $x$-$y$ planes. $\varepsilon$, $\sigma$, $D$ and $E$ are the strain, stress, electrical displacement (charge per unit area) and the electrical field (voltage per unit length) respectively. In addition, $C$, $d$ and $\xi$ are the elastic compliance, the piezoelectric strain constant and the permittivity of the material respectively.

Note that Equation 1.a simply states that the strain of a piezoelectric transducer is given by the sum of the strain due to the mechanical stress and the strain due to the applied electrical field.

The piezoelectric strain constants $d_{mi}$ are defined as the ratio of developed free strain to the applied electric field in the corresponding directions. In the general case the piezoelectric strain tensor can be put in a 6x3 matrix. Of those 18 constants, some may be equal, null or simply related to each other depending on the particular material. In the particular case of interest, electrical charge is applied along the poling direction; constants $d_{33}$, $d_{31}$ and $d_{32}$ are considered and the last two constants are assumed to be equal and related to the first by the Poisson effect. That is the same as assuming the material behaves in the same way along directions 1 and 2.

As mentioned earlier, in the following discussion the electrical field is restricted to be relatively small so that piezoelectric material can be considered linear and thus Equation 1 may be applied.

In the absence of an applied stress, the strain of the piezoelectric element, for the one-dimensional case, may be written as:

$$\varepsilon_3^f = d_{33} \cdot E_3 = \frac{d_{33} \cdot V}{t} \tag{2}$$

where $V$ is the applied voltage, $t$ is the thickness of the material in the $z$ direction and the superscript $f$ refers to the free or unconstrained case.
For the same applied field the actuator will also deform in the $x$ and $y$ direction and the resultant strains are given by:

$$\varepsilon_1^f = \frac{d_{31} \cdot V}{t} \tag{3.a}$$

$$\varepsilon_2^f = \frac{d_{32} \cdot V}{t} \tag{3.b}$$

## 3. Piezoelectric One-Dimensional Perfect Bonded Wafer Configurations

In the one-dimensional case, a free piezoelectric element (assumed to be polarized along the $z$ direction) is assumed to develop compressive or tensional strain in the $x$ direction when activated by applying a voltage in that direction. The induced strain for each direction is determined by the sign and amplitude of the applied voltage and the piezoelectric strain constants of the material.

$$\varepsilon^f = \varepsilon_1^f = \frac{d_{31} \cdot V}{t} = d_{31} \cdot E \tag{4}$$

where $E$ is the electrical field (voltage per unit length).
A piezoelectric actuator may be bonded to a structure in different configurations to form a so-called wafer configuration.
When a voltage is applied across the bonded piezoelectric element it will attempt to expand/contract but will be constrained somewhat due to the stiffness of the beam.
Two common forms of arrangement of a piezoelectric actuator are the two-sided and the one-sided wafer configurations as shown in Figures 2 and 3.
When piezoactuators are activated, surface traction/compression is generated at the piezoactuator/beam interface. If the applied voltage varies sinusoidally with time, the substructure experiences harmonic excitation. An important assumption is that the beam is covered by a piezoelectric material, which is perfectly bonded to the beam. The following derivation is an approximation using a static approach; inertial effects of the piezoelectric element are ignored, which is valid if the element is thin and lightweight compared to the beam substructure or at low frequencies.
Given a combined structure (wafer) that is thin compared to radius of curvature, a linear strain distribution can be assumed across the thickness direction [12] and therefore the strains at each of the interfaces will be continuous:

$$\varepsilon(z) = k \cdot z + \varepsilon_0 \tag{5}$$

where $k$ is the strain slope and $\varepsilon_0$ is the $z$ intercept as sketched in Figure 4.

Using the strain distribution and Hook's law, the stress distribution within the beam is given by:

$$\sigma_b = Y_b \cdot (k \cdot z + \varepsilon_0) \tag{6}$$

where $Y_b$ is the Young's modulus of the beam.
The stress distribution within the piezoelectric actuator is a function of the unconstrained strain, the Young's elastic modulus of the piezoelectric material and the assumed strain distribution as shown by:

$$\sigma_p = Y_p \cdot (k \cdot z + \varepsilon_0 \pm \varepsilon^f) \tag{7}$$

where $Y_p$ is the Young's modulus of the piezoelectric material, $\varepsilon^f$ is the unconstrained strain and the +/- sign applies if tension or compression is respectively induced into the piezoelectric element. Note that if the piezoelectric element is forced to expand, a compressive state is induced in it due to the stiffening effect of the beam, while if it is forced to contract a tensile state is induced instead.

# 4. Two-Sided Wafer Configuration

In this configuration, actuators are symmetrically bonded on the upper and lower surface of a beam (Figure 2). If both actuators are arranged to generate surface strain of opposite sign (out-of-phase actuation), the beam will experience bending forces and out-of-plane or flexural vibration is induced. If both actuators are arranged to generate surface strain of equal sign (in-phase actuation), the beam will experience compressional forces and in-plane vibration is induced.

## *4.1. Out-of-phase Excitation: Effective Moment*

In the absence of externally applied forces and moments, there must be force and moment equilibrium at all sections of the beam/actuator structure. Thus applying these two conditions we get two equations in the unknowns $k$ and $\varepsilon_0$.
According to Equations 6 and 7, the following relations give stresses in the beam and actuators:

$$\sigma_b = Y_b \cdot (k \cdot z + \varepsilon_0) \tag{8.a}$$

$$\sigma_{p1} = Y_p \cdot (k \cdot z + \varepsilon_0 + \varepsilon^f) \tag{8.b}$$

$$\sigma_{p2} = Y_p \cdot (k \cdot z + \varepsilon_0 - \varepsilon^f) \tag{8.c}$$

Applying moment and force equilibrium conditions gives the following equations:

$$\int_{-\frac{t_b}{2}-t_p}^{-\frac{t_b}{2}} \sigma_{p1} \cdot z \cdot dz + \int_{-\frac{t_b}{2}}^{\frac{t_b}{2}} \sigma_b \cdot z \cdot dz + \int_{\frac{t_b}{2}}^{\frac{t_b}{2}+t_p} \sigma_{p2} \cdot z \cdot dz = 0 \tag{9.a}$$

$$\int_{-\frac{t_b}{2}-t_p}^{-\frac{t_b}{2}} \sigma_{p1} \cdot dz + \int_{-\frac{t_b}{2}}^{\frac{t_b}{2}} \sigma_b \cdot dz + \int_{\frac{t_b}{2}}^{\frac{t_b}{2}+t_p} \sigma_{p2} \cdot dz = 0 \tag{9.b}$$

where $t_b$ and $t_p$ are the thickness of the beam and the piezoactuator respectively, as shown in Figure 4. Equations 9.a and 9.b are solved to give:

$$k = \frac{12 \cdot \varepsilon^f \cdot t_p \cdot (t_b + t_p) \cdot Y_p}{t_b^3 \cdot Y_b + 6 \cdot t_b^2 \cdot t_p \cdot Y_p + 12 \cdot t_b \cdot t_p^2 \cdot Y_p + 8 \cdot t_p^3 \cdot Y_p} = \frac{12 \cdot Y \cdot T \cdot (1+T) \cdot \varepsilon^f}{t_b \cdot (1 + 6 \cdot T \cdot Y + 12 \cdot T^2 \cdot Y + 8 \cdot T^3 \cdot Y)} \tag{10.a}$$

$$\varepsilon_0 = 0 \tag{10.b}$$

where the thickness ratio $T$ and the Young's modulus ratio $Y$ are defined as follows:

$$T = \frac{t_p}{t_b} \qquad Y = \frac{Y_p}{Y_b} \tag{11.a, 11.b}$$

Due to symmetry, the constant $\varepsilon_0$ turns out to be zero.
Figure 5 shows the strain and stress distribution in the wafer structure.
We can thus write an expression for the strain at the actuator/beam interface:

$$\varepsilon^s = \varepsilon\Big|_{z=\frac{t_b}{2}} = C_0 \cdot \varepsilon^f \tag{12}$$

where the superscript '$s$' refers to the 'surface interface' and $C_0$ is a non-dimensional constant given by:

$$C_0 = \frac{6 \cdot Y \cdot T \cdot (1+T)}{1+6 \cdot T \cdot Y + 12 \cdot T^2 \cdot Y + 8 \cdot T^3 \cdot Y} \tag{13}$$

The deformation induced by the actuator to the beam underneath is equivalent to that induced by a moment distribution $M_i$ equal to:

$$M_i = Y_b \cdot I_b \cdot k = Y_b \cdot I_b \cdot \frac{\varepsilon_s}{t_b/2} = C_0 \cdot Y_b \cdot I_b \cdot \frac{\varepsilon^f}{t_b/2} = K_0 \cdot \varepsilon^f \tag{14}$$

where the subscript $i$ stands for 'induced' and the factor $K_0$ emphasizes the fact that the induced moment is proportional to the unconstrained strain $\varepsilon^f$.
The above results are valid for a composite structure where the substructure (beam) is fully covered by the piezoactuators, which are assumed to be perfectly bonded to the beam surfaces.
We now examine the excitation of an infinite thin beam by the action of a two piezoelectric elements of finite extent. For the following derivation further assumptions are made. It is assumed that the piezoelectric element is very long and thin and hence edge effects are ignored. Free edges do actually exist where the stress field vanish and the equilibrium conditions require the normal stress at the actuator boundaries to be zero, invalidating the above relationships. The assumption made is supported by the work of Liang and Rogers [8], who showed that the actuator stress field for a distributed actuator is unaffected by the free edge except within approximately four actuator thickness distances from the boundaries. Thus for a large piezoactuator patch (with respect to the actuator thickness) the stress field is largely unaffected by the free boundaries. Consequently, the stress field described above generates a bending moment, which is assumed to be uniform within the boundaries of the piezoactuators.
Thus the flexural response of the beam associated with the induced moment field is solved. The Bernoulli-Euler equation for a thin beam including the actuator-induced moment is given by [9]:

$$\frac{\partial^2 [M(x) - M_i(x)]}{\partial x^2} - \rho A \frac{\partial^2 w}{\partial t^2} = 0 \tag{15}$$

where $M(x)$ and $M_i(x)$ are the internal beam bending moment and the induced actuator bending moment respectively, while $\rho$, $A$ and $w(x,t)$ are the beam density, cross sectional area and out-of-plane displacement respectively.
For a finite length element, the moment $M_i(x)$ may be written as follow:

$$M_i(x) = K_0 \cdot \varepsilon^f \cdot [H(x) - H(x - L_p)] \tag{16}$$

where $Lp$ is the actuator length and $H$ () is the Heaviside step function defined as:

$$H(x) = \begin{cases} 1, x > 0 \\ 0, x < 0 \end{cases} \tag{17}$$

This implies that the induced moment exists at every point under the piezoelectric element.

If a harmonic oscillating voltage $V=Ve^{j\omega t}$ of circular frequency $\omega$ is applied across the piezoelectric element electrodes and a harmonic solution $w=We^{j\omega t}$ is assumed, by substituting the moment distribution expression given by Equation 16 into Equation 15 and rearranging we get:

$$YI\frac{d^4W}{dx^4} - \omega^2 \rho AW = K_0 \cdot \varepsilon^f \cdot [\delta'(x) - \delta'(x - L_p)] \tag{18}$$

where all properties refer to the beam and subscript '*b*' is omitted for simplicity. $\delta'$ () represents the derivative of the Dirac delta function. Equation 18 shows that the induced bending of the actuators may be represented as an external load consisting of a pair of line moments of opposite sign located at the actuator edges (Figure 6) as described by Fansen [10] and Crawley [11].

The final expression for the effective bending moment (Equation 14) is a function of the thickness and material properties of the beam and the piezoelectric elements. It also depends on the free actuator strain $\varepsilon^f$ and thus is proportional to the applied electric field *E*.

It is interesting to examine the strain induced by the piezoelectric patches to see if there is an optimal thickness for the piezoelectric elements, which maximizes the induced strain itself and thus the induced moment.

We therefore define the strain ratio *R* to be the strain at the interface divided by the free piezoactuator strain:

$$R = \frac{\varepsilon^s}{\varepsilon^f} = C_0 = \frac{6 \cdot Y \cdot T \cdot (1+T)}{1 + 6 \cdot T \cdot Y + 12 \cdot T^2 \cdot Y + 8 \cdot T^3 \cdot Y} \tag{19}$$

This equation is plotted (Figures 7-8) for steel and aluminium beams as a function of the thickness ratio. Material properties are specified in Table 1.

| Property | PZT (PC5H) Type V1 | Aluminium | Steel |
|---|---|---|---|
| Young's Modulus ($Nm^{-2}$) | $59.5 \times 10^9$ | $70 \times 10^9$ | $210 \times 10^9$ |

Table 1 – Material properties

As shown in Figures 7 and 8, there is an optimal thickness ratio that depends on the substructure material. The strain ratio tends to zero as the thickness ratio becomes very large which is consistent with the fact that if the thickness of the piezoactuators is very large compared to the beam thickness and they are driven out-of-phase, they act against each other and the thin layer in between (the beam) does not experience any excitation.

## *4.2. In-phase Excitation: Effective Force*

With reference to Figure 9, in the absence of externally applied forces and moments, there must be force and moment equilibrium at all sections of the beam/actuator structure. Thus applying those two conditions results in two equations with the unknowns $\varepsilon_0$ and k, which turns out to be zero by symmetry.

The following relations give stresses in the beam and actuators:

$$\sigma_b = Y_b \cdot (k \cdot z + \varepsilon_0) \tag{20.a}$$

$$\sigma_{p1} = Y_p \cdot (k \cdot z + \varepsilon_0 - \varepsilon^f) \tag{20.b}$$

$$\sigma_{p2} = Y_p \cdot (k \cdot z + \varepsilon_0 - \varepsilon^f) \tag{20.c}$$

By applying moment and force equilibrium conditions, Equation 9 can be solved for *k* and $\varepsilon_0$ to give the following:

$$k = 0 \tag{21.a}$$

$$\varepsilon_0 = \frac{2 \cdot \varepsilon^f \cdot t_p \cdot Y_p}{t_b \cdot Y_b + 2 \cdot t_p \cdot Y_p} = \frac{2 \cdot T \cdot Y \cdot \varepsilon^f}{1 + 2 \cdot T \cdot Y} \tag{21.b}$$

Figure 9 shows the strain and stress distribution in the wafer structure.
As in the previous section, $T$ is defined as the thickness ratio and $Y$ as the Young's modulus ratio. An expression for the uniform strain induced in the actuator/beam structure is given by:

$$\varepsilon^s = \varepsilon_0 = \frac{2 \cdot T \cdot Y \cdot \varepsilon^f}{1 + 2 \cdot T \cdot Y} = C_1 \cdot \varepsilon^f \tag{22}$$

The superscript '$s$' is again used to represent the surface, as for the previous case. Note that now the strain is constant over the beam cross-section, and $C_1$ is a non-dimensional constant given by:

$$C_1 = \frac{2 \cdot T \cdot Y}{1 + 2 \cdot T \cdot Y} \tag{23}$$

The longitudinal response of the beam associated with the induced strain field can thus be solved. The longitudinal equation of motion for a beam is given by:

$$\rho A \frac{\partial^2 u}{\partial t^2} = A \frac{\partial \sigma}{\partial x} \tag{24}$$

where $u(x,t)$ is the in-plane displacement and $\sigma$ is the stress field, which can be written as:

$$\sigma = Y \cdot \left( \frac{\partial u}{\partial x} - \varepsilon^s \right) \tag{25}$$

Combining Equations 24 and 25 gives:

$$Y \frac{\partial^2 u}{\partial x^2} - \rho \frac{\partial^2 u}{\partial t^2} = Y \frac{d\varepsilon^s}{dx} \tag{26}$$

For a finite length element, $\varepsilon^f$ may be written as:

$$\varepsilon^f(x) = C_1 \cdot \varepsilon^f \cdot [H(x) - H(x - L_p)] \tag{27}$$

If a harmonic oscillating voltage $V = Ve^{j\omega t}$ of circular frequency $\omega$ is applied across the piezoelectric element electrodes and a harmonic solution $u = Ue^{j\omega t}$ is assumed, by substituting the strain distribution expression given by Equation 27 into Equation 26 and rearranging we get:

$$Y \frac{d^2 u}{dx^2} + \omega^2 \rho \cdot u = Y \cdot C_1 \cdot \varepsilon^f \cdot [\delta(x) - \delta(x - L_p)] \tag{28}$$

Equation 28 shows that the induced force of the actuators may be represented as an external load consisting of a pair of line forces of opposite sign located at the actuator edges and acting in the $x$

direction (Figure 11). The magnitude of these forces is proportional to the applied voltage by the factor $K_1$.

$$F_i = A_b \cdot Y_b \cdot \varepsilon^s = C_1 \cdot A_b \cdot Y_b \cdot \varepsilon^f = K_1 \cdot \varepsilon^f \tag{29}$$

The final expression for the effective force (Equation 29) is a function of the thickness and material properties of the beam and the piezoelectric material. It also depends on the free actuator strain $\varepsilon^f$ and thus is proportional to the applied electric field.
It is interesting to examine the strain induced by the piezoelectric patches. It can be seen that in this case no optimal thickness exists. We define the strain ratio to be the uniform strain in the structure divided by the free piezoactuator strain:

$$R = \frac{\varepsilon^s}{\varepsilon^f} = C_1 = \frac{2 \cdot T \cdot Y}{1 + 2 \cdot T \cdot Y} \tag{30}$$

Equation 30 is plotted in Figure 11 for steel and aluminium beams as a function of the thickness ratio.

## 5. One-Sided Wafer Configuration

In this configuration, the actuator is bonded on the surface of a beam as shown in Figure 3. When a voltage is applied to the actuator, surface strain is induced on the beam. All the assumptions made for the previous cases are implicitly assumed here as well as a linear strain distribution (Equation 5). The stresses in the beam and actuator are given by:

$$\sigma_b = Y_b \cdot (k \cdot z + \varepsilon_0) \tag{31.a}$$

$$\sigma_p = Y_p \cdot (k \cdot z + \varepsilon_0 - \varepsilon^f) \tag{31.b}$$

Applying moment and force equilibrium conditions gives the following equations:

$$\int_{-\frac{t_b}{2}}^{\frac{t_b}{2}} \sigma_b \cdot z \cdot dz + \int_{\frac{t_b}{2}}^{\frac{t_b}{2}+t_p} \sigma_p \cdot z \cdot dz = 0 \tag{32.a}$$

$$\int_{-\frac{t_b}{2}}^{\frac{t_b}{2}} \sigma_b \cdot dz + \int_{\frac{t_b}{2}}^{\frac{t_b}{2}+t_p} \sigma_p \cdot dz = 0 \tag{32.b}$$

Which are solved to give:

$$k = \frac{6 \cdot \varepsilon^f \cdot t_b \cdot t_p \cdot (t_b + t_p) \cdot Y_p \cdot Y_b}{t_b^4 \cdot Y_b^2 + 4 \cdot t_b^3 \cdot t_p \cdot Y_b \cdot Y_p + 6 \cdot t_b^2 \cdot t_p^2 \cdot Y_p \cdot Y_b + 4 \cdot t_b \cdot t_p^3 \cdot Y_p \cdot Y_b + t_p^4 \cdot Y_p^2} = \tag{33.a}$$

$$= \frac{6 \cdot Y \cdot T \cdot (1+T) \cdot \varepsilon^f}{t_b \cdot (1 + 4 \cdot T \cdot Y + 6 \cdot T^2 \cdot Y + 4 \cdot T^3 \cdot Y + T^4 \cdot Y^2)}$$

$$\varepsilon_0 = \frac{\varepsilon^f \cdot t_p \cdot (t_b^3 \cdot Y_b + t_p^3 \cdot Y_p) \cdot Y_p}{t_b^4 \cdot Y_b^2 + 4 \cdot t_b^3 \cdot t_p \cdot Y_b \cdot Y_p + 6 \cdot t_b^2 \cdot t_p^2 \cdot Y_p \cdot Y_b + 4 \cdot t_b \cdot t_p^3 \cdot Y_p \cdot Y_b + t_p^4 \cdot Y_p^2} = \tag{33.b}$$

$$= \frac{Y \cdot T \cdot (1 + T^3 \cdot Y) \cdot \varepsilon^f}{1 + 4 \cdot T \cdot Y + 6 \cdot T^2 \cdot Y + 4 \cdot T^3 \cdot Y + T^4 \cdot Y^2}$$

Figure 12 shows the strain and stress distribution in the wafer structure.
The surface strain at the actuator/beam interface is given by:

$$\varepsilon^s = \varepsilon\Big|_{z=\frac{t_b}{2}} = \frac{Y \cdot T \cdot (4 + 3 \cdot T + T^3 \cdot Y) \cdot \varepsilon^f}{1 + 4 \cdot T \cdot Y + 6 \cdot T^2 \cdot Y + 4 \cdot T^3 \cdot Y + T^4 \cdot Y^2} = C_0 \cdot \varepsilon^f \tag{34}$$

Due to asymmetry in this case, the strain distribution can be decomposed into the sum of a symmetric distribution $k \cdot z$ (flexural component) and a uniform strain distribution $\varepsilon_0$ (longitudinal component) as shown in Figure 13.
Thus the response of the beam to the actuator consists of the sum of a linear strain distribution (equivalent moment) and a uniform strain distribution (equivalent force). The effective force and moment are given, following the earlier analysis, by:

$$M_i = Y_b \cdot I_b \cdot k = C_2 \cdot Y_b \cdot I_b \cdot \frac{\varepsilon^f}{t_b/2} = K_2 \cdot \varepsilon^f \tag{35.a}$$

$$F_i = A_b \cdot Y_b \cdot \varepsilon_0 = C_3 \cdot Y_b \cdot A_b \cdot \varepsilon^f = K_3 \cdot \varepsilon^f \tag{35.b}$$

where:

$$C_2 = \frac{3 \cdot Y \cdot T \cdot (1+T)}{1+4 \cdot T \cdot Y + 6 \cdot T^2 \cdot Y + 4 \cdot T^3 \cdot Y + T^4 \cdot Y^2} \tag{36.a}$$

$$C_3 = \frac{Y \cdot T \cdot (1+T^3 \cdot Y)}{1+4 \cdot T \cdot Y + 6 \cdot T^2 \cdot Y + 4 \cdot T^3 \cdot Y + T^4 \cdot Y^2} \tag{36.b}$$

Previous results for flexural and longitudinal vibration can be used and superposition may be applied to find the total response of the system.
It is interesting to examine again the strain induced by the piezoelectric patches to see if there is an optimal thickness for the piezoelectric element. We thus define the strain ratio as before:

$$R = \frac{\varepsilon^s}{\varepsilon^f} = \frac{Y \cdot T \cdot (4+3 \cdot T + T^3 \cdot Y)}{1+4 \cdot T \cdot Y + 6 \cdot T^2 \cdot Y + 4 \cdot T^3 \cdot Y + T^4 \cdot Y^2} \tag{37}$$

This equation is plotted (Figures 14-15) for steel and aluminium beams as a function of the thickness ratio.
As shown in Figures 14 and 15, there is an optimal thickness ratio for $T$ less than one and it depends on the substructure material. As shown in Figure 15, the strain ratio tends to unity as the thickness ratio becomes very large. This is consistent with the fact that if the thickness of the piezoactuator is very large compared to the beam thickness, the strain of the piezoelectric element will not be affected by the relatively light stiffening effect of the beam.
It is also interesting to note that the values of $M_i$ and $F_i$ for this case are not exactly half of the results found out in the earlier sections. This fact arises because the expression of the single actuator does not include the stiffening effect of the second actuator. If this stiffness is included in the analysis and a zero voltage is applied to that element, it is shown that the results are exactly half of that for the two-patch actuators. If that is indeed the case, the stress distribution in the beam and piezoelectric element may be written as follows:

$$\sigma_b = Y_b \cdot (k \cdot z + \varepsilon_0) \tag{38.a}$$

$$\sigma_{p1} = Y_p \cdot (k \cdot z + \varepsilon_0 + 0) \tag{38.b}$$

$$\sigma_{p2} = Y_p \cdot (k \cdot z + \varepsilon_0 - \varepsilon^f) \tag{38.c}$$

By applying equilibrium conditions (Equation 9) and solving for $k$ and $\varepsilon_0$ we end up with:

$$k = \frac{6 \cdot \varepsilon^f \cdot t_p \cdot (t_b + t_p) \cdot Y_p}{t_b^3 \cdot Y_b + 6 \cdot t_b^2 \cdot t_p \cdot Y_p + 12 \cdot t_b \cdot t_p^2 \cdot Y_p + 8 \cdot t_p^3 \cdot Y_p} = \frac{6 \cdot Y \cdot T \cdot (1+T) \cdot \varepsilon^f}{t_b \cdot (1+6 \cdot T \cdot Y + 12 \cdot T^2 \cdot Y + 8 \cdot T^3 \cdot Y)}$$

$$\varepsilon_0 = \frac{\varepsilon^f \cdot t_p \cdot Y_p}{t_b \cdot Y_b + 2 \cdot t_p \cdot Y_p} = \frac{T \cdot Y \cdot \varepsilon^f}{1+2 \cdot T \cdot Y}$$

Which are half of the corresponding expressions for the two-sided wafer configuration when actuators are driven out-of-phase and in-phase respectively. The effective force and moment are given by:

$$M_i = C_4 \cdot Y_b \cdot I_b \cdot \frac{\varepsilon^f}{t_b/2} = K_4 \cdot \varepsilon^f \tag{40.a}$$

$$F_i = C_5 \cdot Y_b \cdot A_b \cdot \varepsilon^f = K_5 \cdot \varepsilon^f \tag{40.b}$$

where:

$$C_4 = \frac{C_0}{2} \tag{41.a}$$

$$C_5 = \frac{C_1}{2} \tag{41.b}$$

# Conclusions

Detailed one-dimensional models of the coupling between piezoelectric actuators and a beam to which they are bonded has been presented and reviewed in this report. Strain and stress distribution within the actuators and the beam has been determined by applying the equilibrium conditions. For each case an expression for the effective load is presented and it has been shown to depend on the coupling and on the actuator properties. For some of the configurations, there is an actuator/beam thickness ratio that maximize the effective load. This depends on the actuator/beam Young's modulus ratio.

# References


[1] K. Uchino, *"Ferroelectric Devices"*, Marcel Dekker, Inc, 2000.

[2] D. J. Warkentin, E. F. Crawley, *"Embedded electronics for intelligent structures"*, 32nd Conference on Structures, Structural Dynamics, and Materials, Proceedings of AIAA/ASME/ASCE/AHS/ASC, pp. 1322-1331, Baltimore, MD, USA, Apr. 1991

[3] C. A. Rosen, *"Analysis and Design of Ceramic Transformers and Filter Elements"*, Ph. D. Dissertation, Electrical Engineering Dept. Syracuse University, August 1956.

[4] C. A. Rosen, *"Ceramic Transformers and Filters"*, Proc. Of Electronic Comp. Symp., 1956.

[5] C. Y. Lin, *"Design and Analysis of Piezoelectric Transformer Converters"*, Ph.D. Dissertation, Virginia Tech, July 1997.

[6] C. R. Fuller, S. J. Elliot, P. A. Nelson, *"Active Control of Vibration"*, Academic Press, 1996.

[7] S. J. Kim and J. D. Jones, *"Optimal Design of Piezoactuator for Active Noise and Vibration Control"*, AIAAA Journal, Vol. 29, No.12, pp. 2047-2053, December 1991.

[8] C. Liang, C. A. Rogers, *"Behaviour of a Shape Memory Alloy Actuator Embedded in Composites"*, Proceedings of the 1989 International Composite Conference, Beijing, China, August 1989.

[9] W. T. Thomson, *"Theory of Vibration with Applications"*, Prenice-Hall, Inc, 1972.

[10] J. L. Fansen and J. C. Chen, *"Structural Control by the Use of Piezoelectric Active Members"*, Proceedings of NASA/DOD Control-Substructure Interaction Conference, NASA CP-2447. Part 2. 1986.

[11] E. F. Crawley and J. Luis, *"Use of Piezoelectric Actuators as Elements of Intelligent Structures"*, AIAA Journal, Vol. 25. No. 10, pp. 1373-1385, January 1987.

[12] R. M. Jones, *"Mechanics of Composite Materials"*, Hemisphere Publishing Company, New York, 1975.

# Table of Figures

# Figures

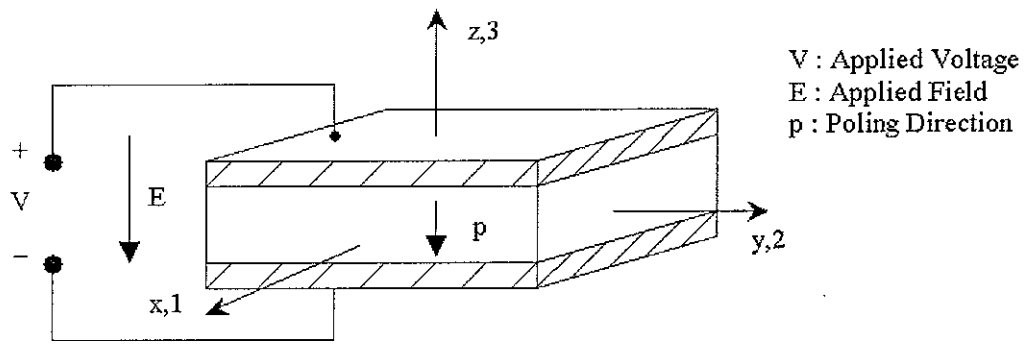


Figure 1 – Convention for direction in a piezoelectric element

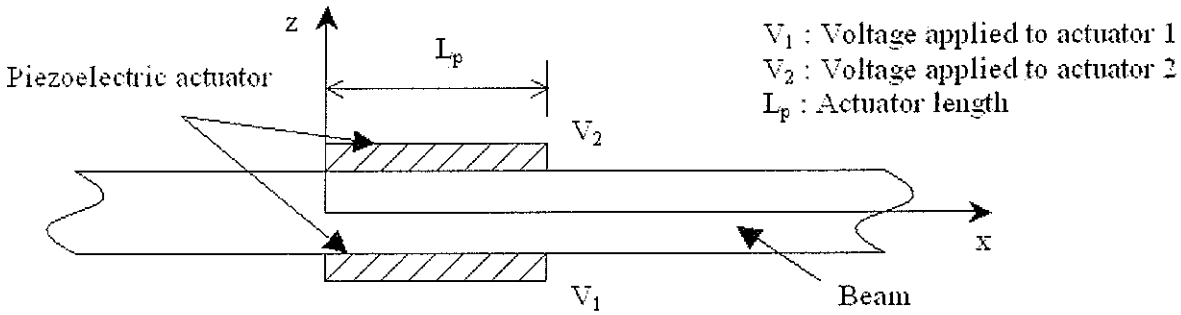


Figure 2 – Two-sided wafer configuration

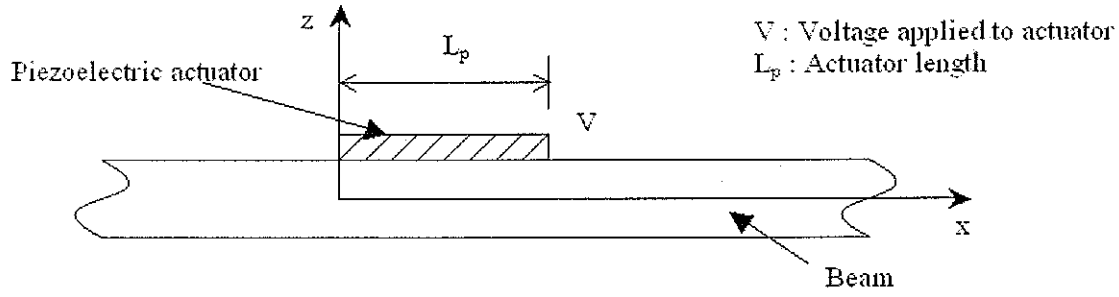


Figure 3 – One-sided wafer configuration

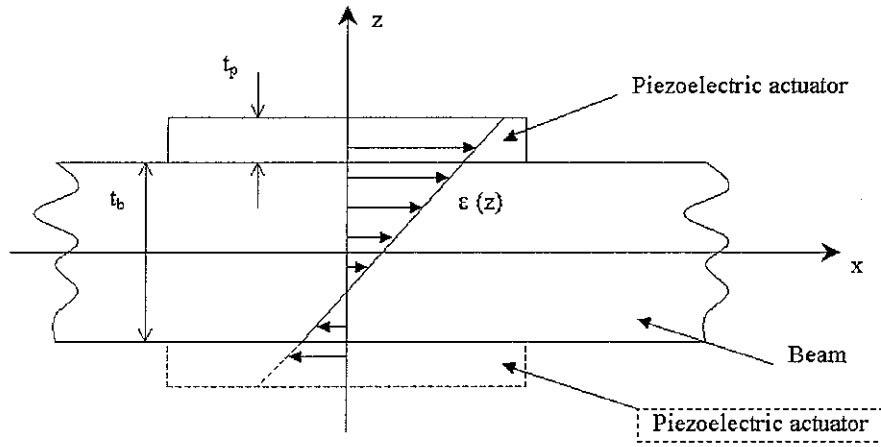


Figure 4 – Assumed Linear strain distribution of a beam and piezoelectric actuators in bending

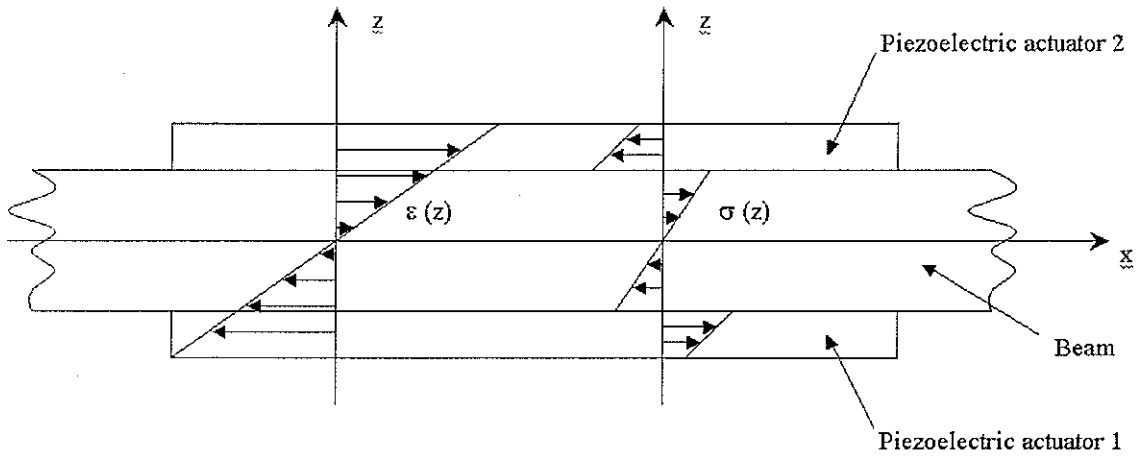


Figure 5 – Strain and stress distribution due to out-of-phase excitation of two piezoelectric actuators bonded to a beam

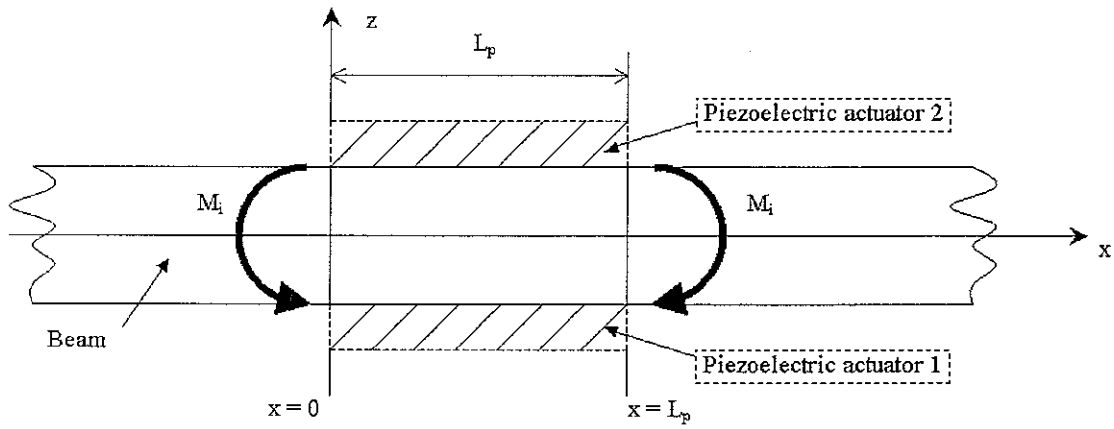


Figure 6 – Equivalent load for out-of-phase excitation

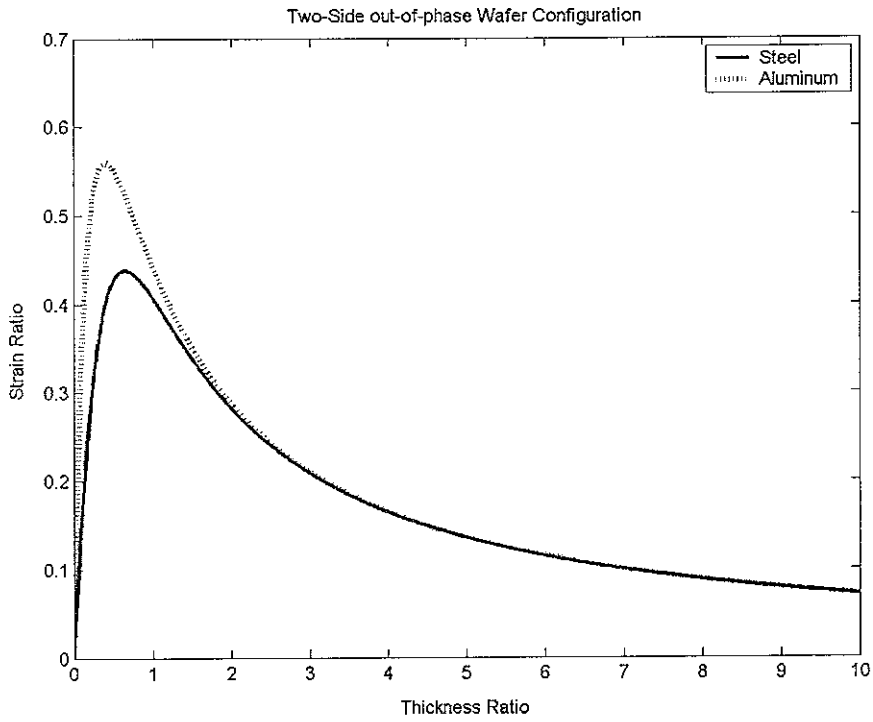


Figure 7 – Strain Ratio as a function of Thickness Ratio for out-of-phase excitation of two piezoelectric actuators

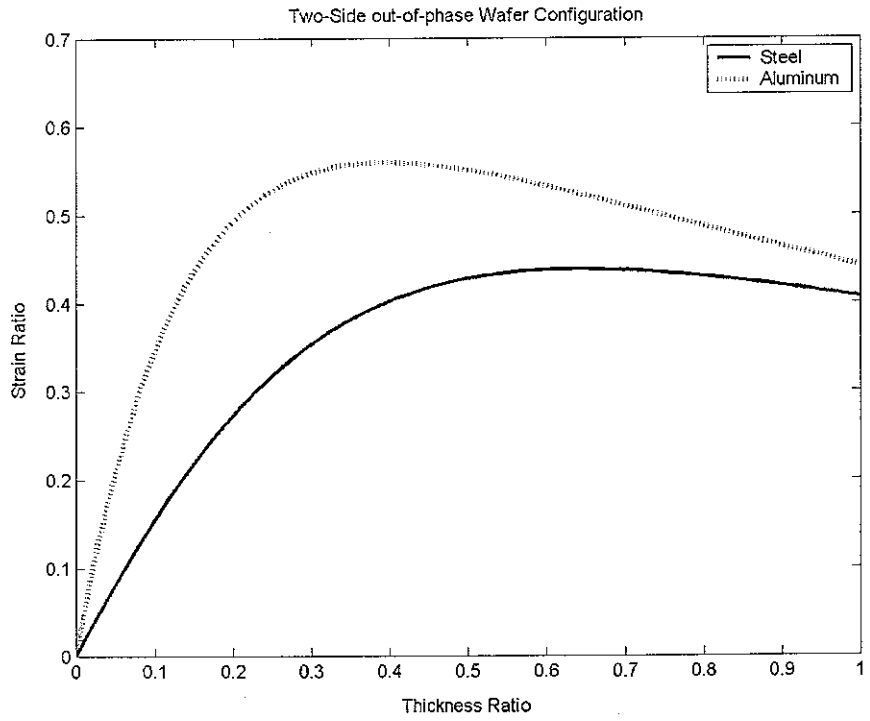


Figure 8 – Strain Ratio as a function of Thickness Ratio, for a Thickness Ratio less than one, for out-of-phase excitation of two piezoelectric actuators

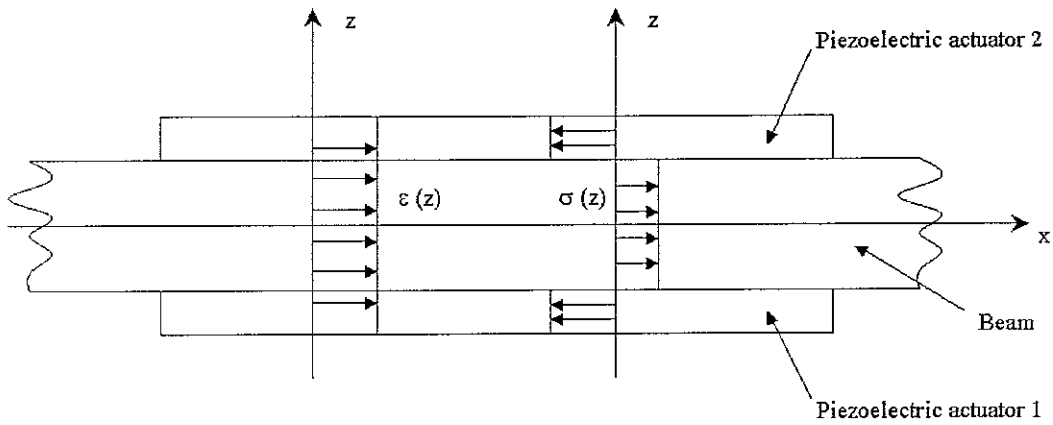


Figure 9 – Strain and stress distribution due to in-phase excitation of two piezoelectric actuators bonded to a beam

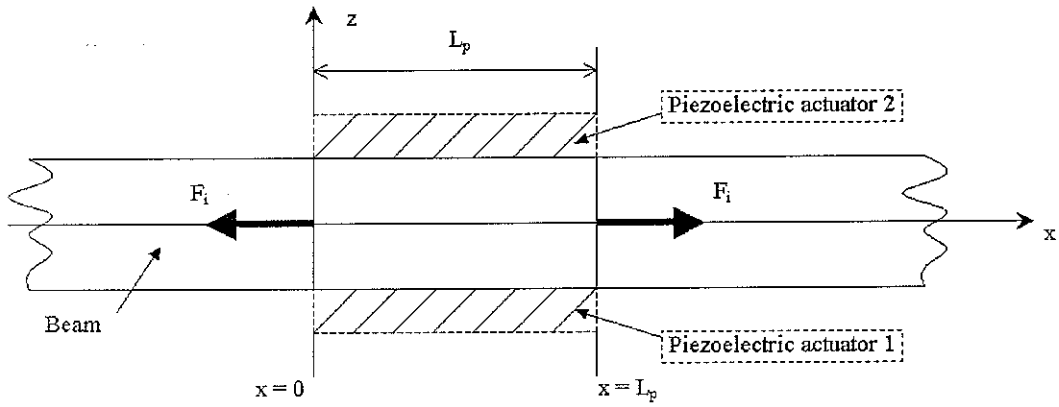


Figure 10 – Equivalent load for in-phase excitation

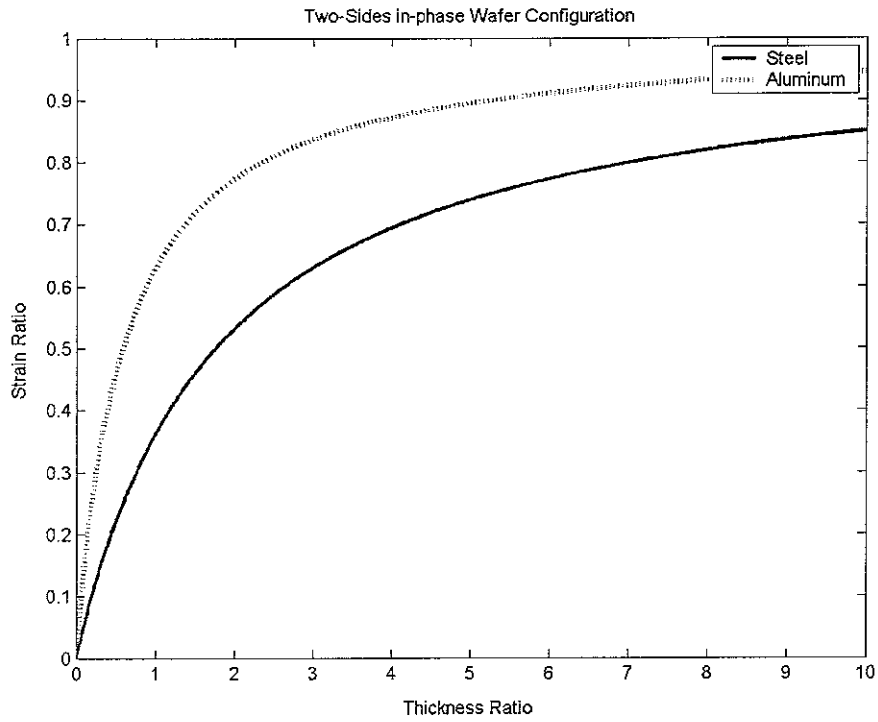


Figure 11 – Strain Ratio as a function of Thickness Ratio for in-phase excitation of two piezoelectric actuators

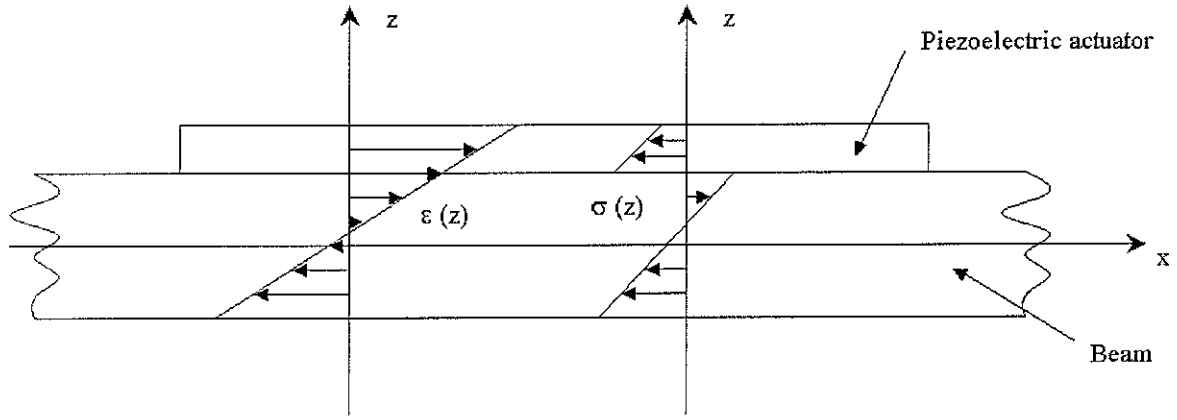


Figure 12 – Strain and stress distribution due to in-phase excitation of one piezoelectric actuator bonded to a beam

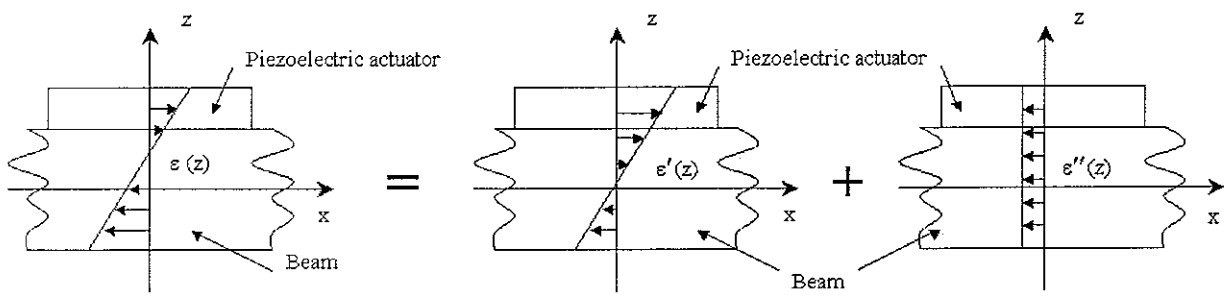


Figure 13 – Asymmetric strain decomposition

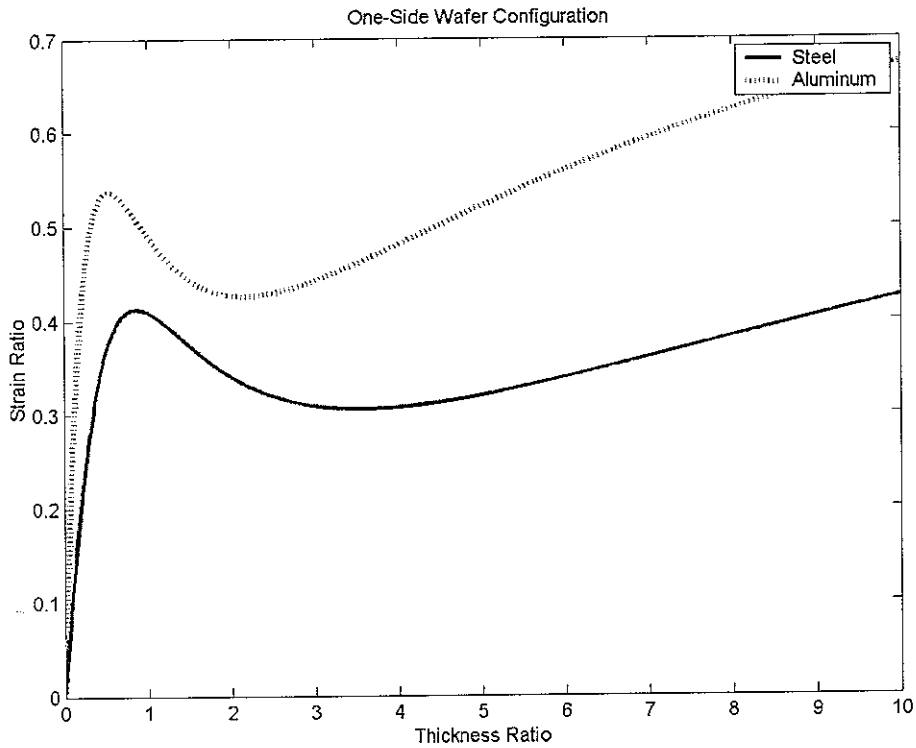


Figure 14 – Strain Ratio as a function of Thickness Ratio for one piezoelectric actuator

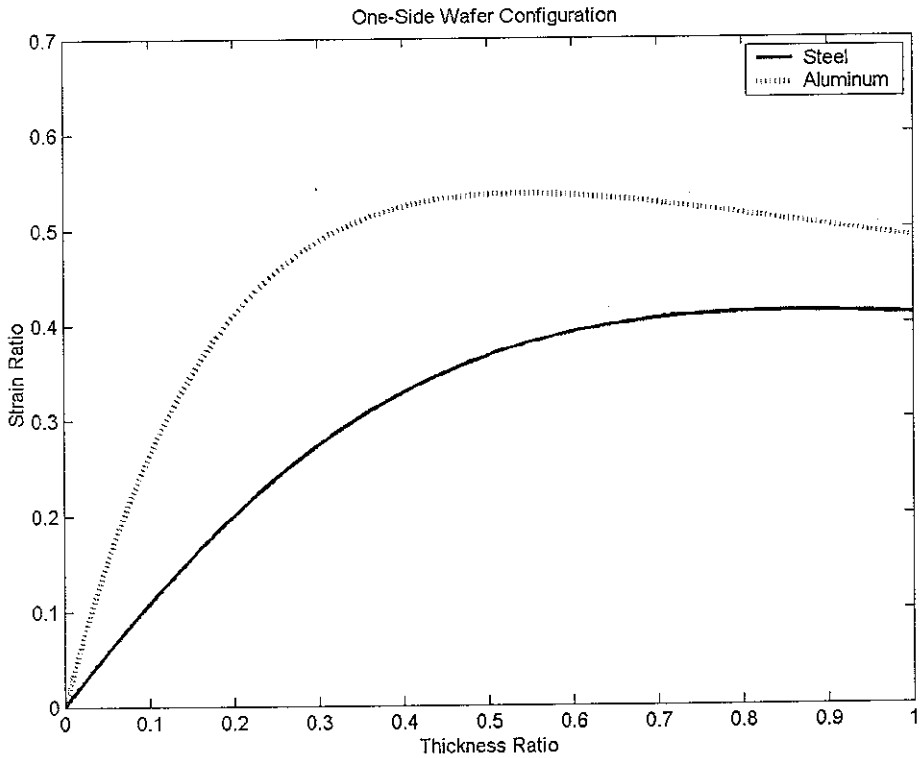


Figure 15 – Strain Ratio as a function of Thickness Ratio, for a Thickness Ratio less than one, for one piezoelectric actuator